


RESEARCH ARTICLE | JANUARY 19 2024

Physical properties of rice husk silica/alumina reinforced aluminium alloy matrix composite produced by cold compaction

Nor Asmalinda Kamaruddin ; Nurul Fitriah Nasir; Noradila Abdul Latif; Mohammad Fikrey Roslan; Nurul Farahin Mohd Joharudin

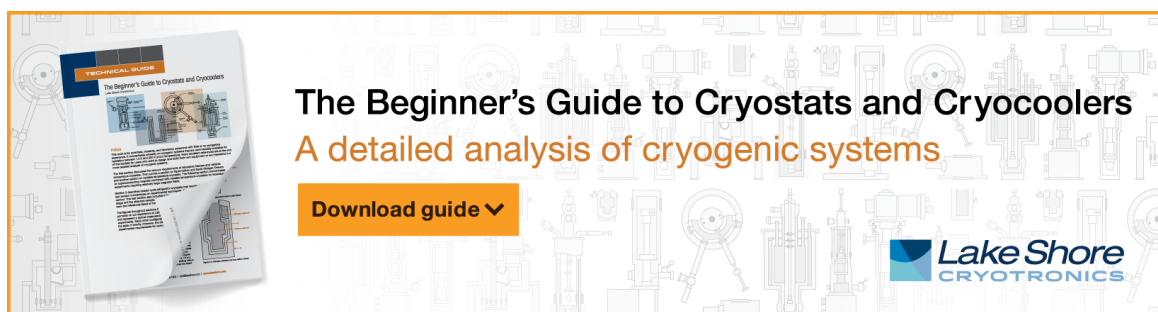


AIP Conf. Proc. 2925, 020050 (2024)

<https://doi.org/10.1063/5.0182817>




CrossMark



The Beginner's Guide to Cryostats and Cryocoolers
A detailed analysis of cryogenic systems

[Download guide](#)



Physical properties of rice husk silica/alumina reinforced aluminium alloy matrix composite produced by cold compaction

Nor Asmalinda Kamaruddin^{1, a)}, Nurul Fitriah Nasir^{1, b)}, Noradila Abdul Latif^{1, c)},
Mohammad Fikrey Roslan^{1, d)}, and Nurul Farahin Mohd Joharudin^{1, e)}

¹*Faculty of Mechanical and Manufacturing Engineering, Universiti Tun Hussien Onn Malaysia, 86400 Parit Raja, Johor, Malaysia*

^{a)} Corresponding author: asmalindakamaruddin@gmail.com

^{b)} fitriah@uthm.edu.my

^{c)} noradila@uthm.edu.my, ^{d)} fikrey.roslan@gmail.com, ^{e)} farahin.joharudin@gmail.com

Abstract. Many researchers are presently investigating the hybridization of aluminium chips due to commercial value, improved properties, and potential applications in aircraft, vehicles, and marine vessel production technologies, as well as to obtain more benefits, such as improved performance, cheaper prices, and less environmental impact. This research examines the effect of alumina (Al₂O₃) and rice husk silica (RHA) as reinforcement on the recycled aluminium alloy (AA7075) chip using the cold compaction process, in which the sample is compressed in a die using a hydraulic press. The aluminium AA7075 chip was reinforced with i.e., 0.5 wt.%, 3.0 wt.%, 5.5 wt.%, 8.0 wt.% and 10.5 wt.% at 63 µm size of RHA, and alumina powder at the sizes of 1.0 µm, 5.0 µm and 35.0 µm. The microstructure images show the random arrangement and various sizes of Al alloy chips in these matrix composite. The density for the sample 0.5RHA/Al₂O₃ reinforced AA7075 with a particle size of 35.0 µm of Al₂O₃ has the highest density at 2.5654 g cm⁻³, while the sample 3.0 RHA/Al₂O₃ reinforced AA7075 with a particle size of 1.0 µm of Al₂O₃ has the lowest of density at 2.3522 g cm⁻³. The porosity and water absorption were inversely proportional to the density. The porosity and water absorption increased until 3.0 wt.% of RHA and decreased to 10.5 wt.% of RHA. The increment of reinforcement composition causes an increase in the porosity due to clustering and pore nucleation between the matrix and reinforcement. However, the water absorption level corresponds with the presence of porosity inside the specimen. Based on investigation, the combination of agro waste and synthetic reinforcement can improve the properties of AMC.

INTRODUCTION

Many researchers are researching the hybridization of aluminium matrix composites because of their commercial value, improved properties, and possible usage in aircraft, automotive, and marine vessel construction. The properties of a composite are affected by its microstructure, capacity, homogeneity, isotropy, particle size, dispersion level, and matrix-particle interface [1, 2].

Reinforcement and particle size impact the AMC composite properties. Typical reinforcing materials include Al₂O₃, AlN, B₄C, TiC, TiB₂, SiC and mica, which enhance tensile strength, wear resistance, hardness, and wear resistance. Alumina is strong and heat-resistant [3]. It can strengthen the microstructure and cause network distortion at the crack tip, which can reduce its breakability [4]. N. Kumar & Soren (2020) state alumina nanoparticles are employed more in research and industry than bulk materials. Density and porosity increase as Al₂O₃ volume percentage and size decrease [5].

Natural materials like bagasse ash, rice husk ash, palm kernel shell ash, bamboo leaf ash, coconut shell ash, and groundnut shell ash (GSA) are used as reinforcement to reduce the costs due to their high silicon dioxide (SiO_2) concentration and low density [6-8]. RHA includes more amorphous silica, carbon, and fewer minerals than slag, silica fume, and fly ash. Silica content determines RHA's industrial efficacy [9]. RHA makes steel. Its low heat conductivity, high melting point, and high porosity make it insulating. An anti-caking agent in toothpaste, cosmetics and food. Silica's hardness is employed in cement and concrete. This additive strengthens bridges and nuclear power plant concrete. Super insulating, catalytic, and dielectric materials use RHA-derived silica adsorbent [10].

This study investigates dual reinforcement's effect on the physical properties of AMC by cold compaction. Powder metallurgy using the cold compaction method is ideally suited for AMC fabrication. This method is widely used due to its low energy consumption, material usage, greater quality, lower cost, low processing temperature, ability to prevent undesired phases, and capacity to produce complex parts compared to other techniques [11-14]. As reported by a previous study, the cold compaction method was proven to improve the properties of AMC. According to Zamani et al., (2021), the cold compaction method provides good properties of AMC with uniform distribution and strong bonding between matrix and reinforcement with no holes. N.F. Mohd Joharuddin et al., (2019) obtained the RHA amorphous silica filled gaps and closed holes in AA7075 aluminium chips to provide a nice surface. Researchers also showed that Al7075 with alumina reinforcement is stronger than Al6061 with SiC reinforcement [15].

MATERIAL AND METHOD

Matrix Materials

An aluminium alloy AA7075 chip is used as the matrix composite for AMCs. Table 1 lists the chemical composition (wt.%) of the AA7075 chip.

TABLE 1. Chemical composition of Aluminium alloy AA7075 chip (wt.%) [16].

| Composition | Al | Zn | Cu | Si | Cr | Others |
|-------------|-------|------|------|------|------|--------|
| Weight (%) | 87.18 | 9.49 | 2.59 | 0.31 | 0.28 | 0.15 |

Reinforced Materials

Rice husk and alumina were used as reinforcing agents in the AMC sample. The rice husk was supplied by the local rice industry, Nano Siltech Sdn. Bhd. The rice husk was transformed into rice husk silica by the burning process as shown in Fig.1. While, alumina in the powder phase is directly bought from Zhengzhou YUFA Abrasives Group Co., Ltd., China. The chemical compositions (in wt.%) of the rice husk silica and Al_2O_3 powder are shown in Table 2 and 3, respectively.

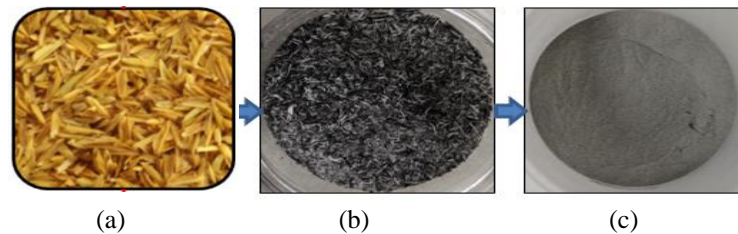


FIGURE 1. a) Raw rice husk [17] b) burned rice husk c) rice husk ash after sieving process

TABLE 2. Rice Husk Silica Composition (wt.%) [16].

| Composition | SiO_2 | SO_3 | Fe_2O_3 | Bal. |
|-------------|----------------|---------------|-------------------------|------|
| Weight (%) | 67.1 | 7.0 | 0.8 | 25.1 |

TABLE 3. Al₂O₃ powder chemical composition (wt.%).

| Composition | O ₂ | Al |
|-------------|----------------|-------|
| Weight (%) | 47.07 | 52.93 |

Preparation of RHA/Al₂O₃ reinforced AA7075 aluminium alloy-based matrix composite

AMC samples were made using a constant alumina of 2.0 wt.% at particle sizes of 1.0 μm, 5.0 μm and 35.0 μm and mixed with different weight percentages of rice husk silica of 0.5wt.%, 3.0wt.%, 5.5wt.%, 8.0wt.%, and 10.5wt.% with 63 μm as shown in Table 4. Zinc stearate at 1% is used as a binder to prevent the agglomeration of mixed compositions.

TABLE 4. AMC sample composition in weight percentages

| AMC Sample | Based matrix | | Reinforcements | |
|------------|----------------------|-------------------------|----------------|--|
| | Al alloy Chip (wt.%) | Rice husk silica (wt.%) | Alumina (wt.%) | |
| 1 | 100.0 | 0 | 0 | |
| 2 | 97.5 | 0.5 | 2.0 | |
| 3 | 95.0 | 3.0 | 2.0 | |
| 4 | 92.5 | 5.5 | 2.0 | |
| 5 | 90.0 | 8.0 | 2.0 | |
| 6 | 87.5 | 10.5 | 2.0 | |

The AMC sample of RHA, Al₂O₃, and AA70775 chips was mixed at 300 rpm for 1 hour by roll milling equipment. This mixing technique provides equal base metal particle dispersion and green, dense compaction. A 9-ton, 20-minute uniaxial hydraulic press compresses the mixture [18]. Compressed powder sinters below the metal’s melting point. Sintering was done in a tube furnace saturated with argon gas for 1 hour. Sintering takes 60 minutes at 552 °C [19]. Around 30 minutes are needed to eliminate the binder (zinc stearate). The compressed AMC sample is sintered according to the sintering profile in Fig.2. In Fig.3, sintered AMC samples with different reinforcement percentages are shown.

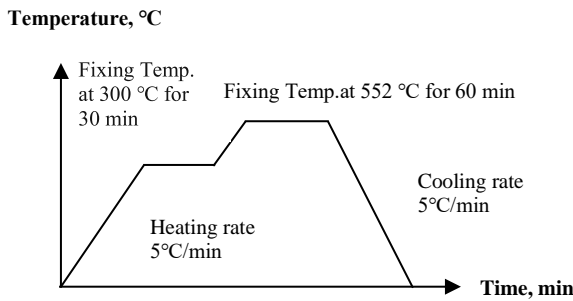


FIGURE 2. Sintering profile [19]

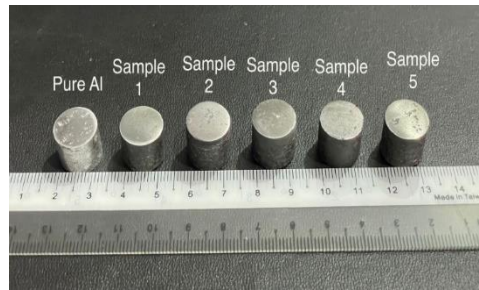


FIGURE 3. Sintered AMC samples

Testing of RHA/Al₂O₃ reinforced AA7075 aluminium alloy-based matrix composite

The RHA/Al₂O₃ reinforced AA7075 matrix composite was tested physically. Optical microscope microstructure analysis (model Olympus BX60M). Physical tests utilising Archimedes’ principles determined density, porosity, and water absorption. Using an electronic balance and density kit, the sample was weighed in air, water, and after soaking (Mettler Toledo, Germany). The density and porosity tests followed ASTM B328 and B962-17.

RESULTS AND DISCUSSION

Microstructural analysis of AMC

The morphology images of the RHA/Al₂O₃ reinforced AA7075 based matrix composites are shown in Fig. 4–6. Significantly, seen of random arrangements and various sizes of Al alloy chips in these matrix composites.

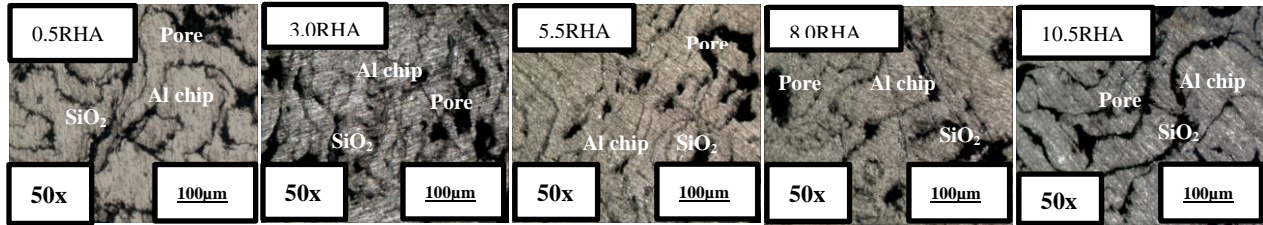


FIGURE 4. Optical Microscope images of AMCs at 1.0 μm

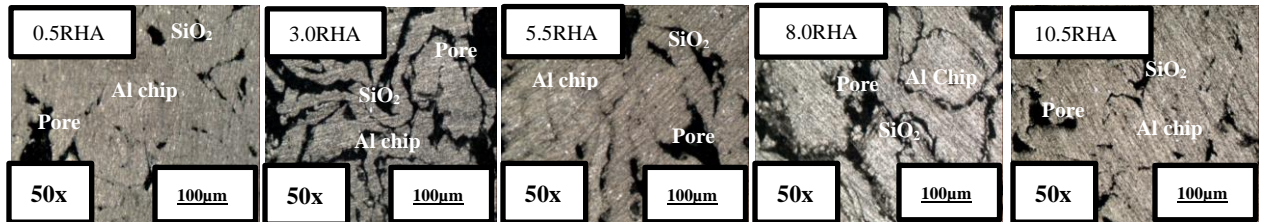


FIGURE 5. Optical Microscope images of AMCs at 5.0 μm

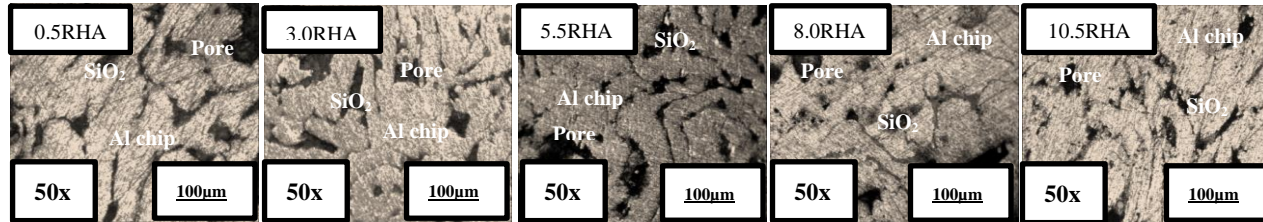


FIGURE 6. Optical Microscope images of AMCs at 35.0 μm

As observed in Fig. 4-6, the images show that many pores had significantly shown up on the surface due to the varying size of the chip. Through the microscope images, it was observed that the pore disappeared when the RHA/Al₂O₃ powder was mixed with the Al chips. The pores on the surface of the sample become smaller.

Microstructure images identified two regions, which are light grey regions, rich in chip content, and dark grey regions, rich in SiO₂ and Al₂O₃ [21]. Porosity appears in the microstructure with non-homogenous agglomeration of RHA and Al₂O₃ particles. This non-homogenous structure increases the number of pores as the density decreases. Furthermore, as the number of powder particles added to the sample increases, the pore formation decreases, becoming smaller in average size and more round in shape [22, 16].

Different sizes of Al₂O₃ particles affect the formation of boundaries. According to Rahimian et al. [20], the interparticle distance between the reinforcements increases as particle size increases, resulting in coarser grains. The formation of intermediate layers at the reinforcement-base metal contact might negatively impact the composite's mechanical characteristics. It has previously been noted that finer particles of a reinforcing phase tend to reduce composite densification. The inter-particle forces become comparatively strong because the van der Waals force predominates between particle bonding when the particle size is sufficiently small. As a result, small particles often limit the powder flowability, lowering the filling density and causing cluster formation [21].

Physical properties of AMC

One of the most well-known tools for assessing the AMC samples' density, apparent porosity, and water absorption is using the Archimedes' principle. Fig. 7 presents the trend of density of the AMC with different compositions of RHA and sizes of alumina as reinforcements.

The density of the pure aluminium chip AA7075 sample obtained from this research was similar to the standard aluminium density at 2.4832 g cm^{-3} . It is apparent from Fig. 7 that the AMC density increased when the particle size of Al_2O_3 increased. The density for the sample 0.5RHA/ Al_2O_3 reinforced AA7075 with a particle size of $35.0 \mu\text{m}$ of Al_2O_3 has the highest density at 2.5654 g cm^{-3} , while the sample 3.0 RHA/ Al_2O_3 reinforced AA7075 with a particle size of $1.0 \mu\text{m}$ of Al_2O_3 has the lowest density at 2.3522 g cm^{-3} . These results indicate that the bulk density is affected by the particle size rather than by volume fraction. This is clarified by the low specific surface and high compressibility of coarse particles [23].

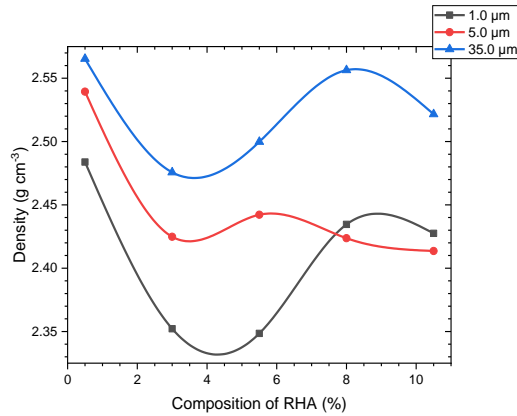


FIGURE 7. Effects of RHA and particle sizes of Al_2O_3 reinforced AA7075 towards density

The presence of low-density RHA has contributed to the decrease in AMC density. This is proven by the rule of mixture [24]. It shows that the reinforcements prevented consolidation during sintering. Alumina's melting temperature is $2054 \text{ }^\circ\text{C}$. The low bonding potential with pure aluminium AA7075 results in a weak network. The reinforcement doesn't fill the space between aluminium particles, reducing the relative density [20]. Fig. 8 and 9 show the porosity and water absorption of AMC made from the different compositions of RHA and alumina sizes as reinforcements.

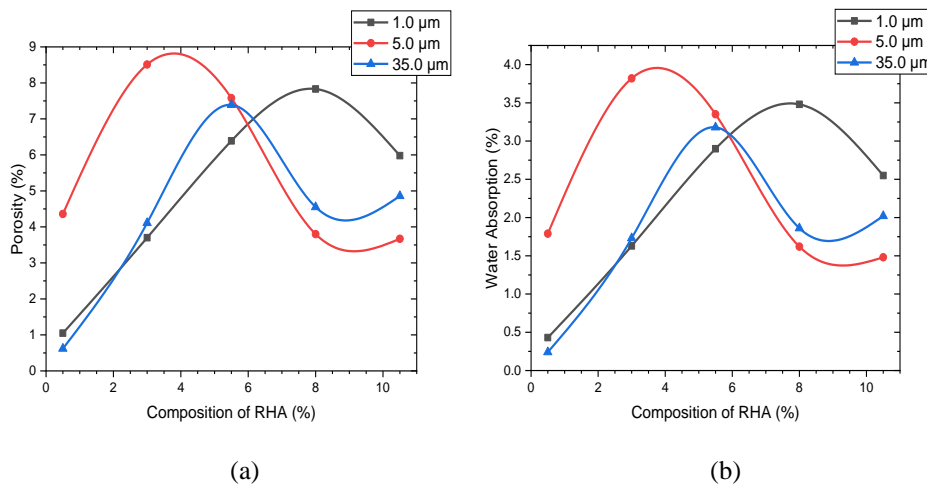


FIGURE 8. Effect of RHA and particle sizes of Al_2O_3 reinforced AA7075 towards a) porosity, b) water absorption

From the graphs in Fig.8 and 9, the porosity and water absorption are inversely proportional to the density of AMCs. The reason for this is the percentage of pores found within a porous solid [22]. The porosity increased until 3.0 wt.% of RHA, and decreased to 10.5 wt.% of RHA. According to Tosun & Kurt (2019), the increment in the reinforcement composition caused by the clustering and pore nucleation also occurs between the matrix and reinforcement, which contributes to increasing the porosity [25].

The porosity is also affected by the sintering temperature and time. When the sintering temperature or duration of the reinforcement was increased, the matrix around the reinforcing material showed enhanced wetting qualities and allowed the powder to flow more readily. Because the powders travel more quickly by diffusion, the phenomena of neck development happen more easily due to the atoms' binding. A denser result is formed. Furthermore, clustering is common when there are a lot of reinforcements [25]. The ability of a sample to absorb water is affected by gravity, which determines how much water it absorbs. However, the water absorption level corresponds with the presence of porosity inside the specimen. According to past research, if the pores rise in the sample, capillary channels rise, thus providing water absorption [26].

CONCLUSION

The physical properties of AMCs reinforced with RHA and Al_2O_3 have been studied. Reinforcement volume fraction and particle size affect the AMCs characteristic. When RHA and Al_2O_3 particles are added to chip, the pore disappears. The Al_2O_3 particle size increased the AMC density. The density inversely affected porosity and water absorption. AMC sample with 0.5% RHA and 35.0 μm Al_2O_3 particle size had increased density, decreased porosity and water absorption. When RHA and Al_2O_3 are added, hybrid aluminium composites work better in aerospace, cars, marine, and electronics.

ACKNOWLEDGMENTS

This research was supported by the Ministry of Higher Education (MOHE) through the Fundamental Research Grant Scheme (FRGS/1/2020/TK03/UTHM/03/17). We also want to thank Universiti Tun Hussein Onn Malaysia for sponsoring this work under research grant No. K067.

REFERENCES

1. P. Garg, Jamwal A., Kumar D., Sadasivuni K. K., Hussain C. M., and Gupta P. [Journal of Materials Research and Technology](#). 8 (2019) 4924-39
2. P. D. Srivyas and Charoo M. S. [Materials Today: Proceedings](#). 5 (2018) 20041-53
3. H. M. Irshad, Hakeem A. S., Ahmed B. A., Ali S., Ali S., Ali S., et al. [International Journal of Refractory Metals and Hard Materials](#). 76 (2018) 25-32
4. P. Bansal and Upadhyay L. [Procedia Technology](#). 23 (2016) 304-10
5. N. Kumar and Soren S. [Materials Today: Proceedings](#). 21 (2020) 1605-09
6. K. K. Alaneme, Ekperusi J. O., and Oke S. R. [Journal of King Saud University - Engineering Sciences](#). 30 (2018) 391-97
7. B. P. Kumar and Birru A. K. [Transactions of Nonferrous Metals Society of China](#). 27 (2017) 2555-72
8. B. Nateq, Haddad-Sabzevar M., Sajjadi S. A., Saba F., Deirmina F., and Pellizzari M. [Composites Communications](#). 25 (2021) 100716
9. R. Pode [Renewable and Sustainable Energy Reviews](#). 53 (2016) 1468-85
10. S. Tiwari and Pradhan M. K. [Materials Today: Proceedings](#). 4 (2017) 486-95
11. G. Abbas Gohar, Manzoor T., and Shah A. N. [Journal of Alloys and Compounds](#). 735 (2018) 802-12
12. S. P. Kumarasamy, Vijayananth K., Thankachan T., and Muthukutti G. P. [Journal of Applied Research and Technology](#). 15 (2017) 430-41
13. J. Liu, Khan U., Coleman J., Fernandez B., Rodriguez P., Naher S., et al. [Materials & Design](#). [94 (2016) 87-94
14. M. Ravikumar, Reddappa H. N., and Suresh R. [Materials Today: Proceedings](#). 5 (2018) 23796-805
15. P. K. Krishnan, Christy J. V., Arunachalam R., Mourad A.-H. I., Muraliraja R., Al-Maharbi M., et al. [Journal of Alloys and Compounds](#). 784 (2019) 1047-61

16. N.F. Mohd Joharudin, N. Abdul Latif, M.S. Mustapa, M.N. Mansor, W.A. Siswanto, J. Murugesan, et al. [Materialwiss Werkstofftech](#). 50 (2019) 1-6
17. N. Soltani, Bahrami A., Pech-Canul M. I., and González L. A. [Chemical Engineering Journal](#). 264 (2015) 899-935
18. A. S. Mahdi, Mustapa M. S., Lajis M. A., and Rashid M. W. A. [International Journal of Science and Research \(IJSR\)](#). 4 (2015) 1759 - 64
19. Mahdi A. S., M. S. Mustapa., Lajis M. A., and Rashid [ARPJ Journal of Engineering and Applied Sciences](#). 11 (2016) 6465-6471
20. M. Rahimian, Parvin N., and Ehsani N. [Materials & Design](#). 32 (2011) 1031-38
21. F. R. Milhorato, Figueiredo R. B., Langdon T. G., and Mazzer E. M. [Journal of Materials Research and Technology](#). 9 (2020) 12626-33
22. M. I. A. Kadir, Mustapa M. S., Latif N. A., and Mahdi A. S. [Procedia Engineering](#). 184 (2017) 687-94
23. F. Aydin [Advanced Powder Technology](#). 32 (2021) 445-63
24. D. S. Prasad, Shoba C., and Ramanaiah N. [Journal of Materials Research and Technology](#). 3 (2014) 79-85
25. G. Tosun and Kurt M. [Composites Part B: Engineering](#). 174 (2019) 106965
26. Y. Wang, Wang W., Wang D., Liu Y., and Liu J. [Journal of Building Engineering](#). 43 (2021) 103120